JOURNAL OF MATERIALS SCIENCE 28 (1993) 6699–6703

Localization of carriers of Y-doped $CaCuO_2$ films prepared by an organometallic-chemical-vapour-deposition method

KENKICHIRO KOBAYASHI, YOZO ISHIHARA, SHIGENORI MATSUSHIMA, GENJI OKADA
Department of Applied Chemistry, Faculty of Engineering, Ehime University, Matsuyama 790, Japan

Y-doped $CaCuO_2$ films have been formed on $SrTiO_3$ (1 0 0) substrates in the range 730–790 °C. The lattice constants of $c = 0.3180 \sim 0.3183$ nm were estimated from the X-ray diffraction (XRD) of *c*-axis-oriented Y-doped $CaCuO_2$ films. The values of the *c*-axis were shorter than those of the undoped $CaCuO_2$ film. Although the resistivity of a Y-doped $CaCuO_2$ film is significantly lower in comparison with that of an undoped $CaCuO_2$ film, no superconductivity was found in these Y-doped $CaCuO_2$ films at temperatures higher than 12 K.

1. Introduction

$CaCuO_2$ with infinite CuO_2 sheets is the parent material in superconductors of a Bi–Sr–Ca–Cu–O and a Tl–Ba–Ca–Cu–O system. In the $CaCuO_2$ structure, an appreciable interaction is probably present between the CuO_2 sheets, so that the correlation of the interaction between the CuO_2 sheets to a T_c value may be revealed from investigation of the superconductivity of $CaCuO_2$. Electron doping of $CaCuO_2$ has been attempted to obtain a superconducting $CaCuO_2$. No one has succeeded , however, in the electron doping of $CaCuO_2$. Recently, Smith *et al.* [1] found superconductivity at 40 K in Nd-doped $SrCuO_2$, with infinite CuO_2 sheets, which was prepared by means of a solid-state reaction at high pressure. They interpreted the failure of electron-doping of $CaCuO_2$ as being due to a small Cu–O bond length as in Gd_2CuO_4 [1]. Another reason may be associated with the instability of $CaCuO_2$ at high pressure, because $CaCuO_2$ has not been prepared at high pressures [2]. Using an organometallic-chemical-vapour-deposition (MOCVD) method, the authors succeeded in the preparation of $CaCuO_2$ [3]; this was not synthesized by the conventional solid-state reaction. The present work attempted the preparation of Y-doped $CaCuO_2$ films by employing the MOCVD method, and the electrical properties of the Y-doped $CaCuO_2$ films were also investigated.

2. Experimental procedure

Chelates of copper, yttrium and calcium with ligands of 2,2,6,6-tetramethyl-3,5-heptanedione (thd) were used as precursors. Y-doped $CaCuO_2$ films were deposited on single crystals of $SrTiO_3$ (1 0 0). The deposition rate was controlled by the sublimation temperatures of the chelates (the sublimation temperatures of $Cu(thd)_2$, $Y(thd)_3$ and $Ca(thd)_2$ were varied in the range 95–105 °C, 160–170 °C and 180–190 °C, respectively). The film preparation was carried out at the total pressure of 100–200 Pa. The thicknesses of the films were measured by means of a surface roughness meter (Kosaka SE-30D). A film deposited for 1 h was about 50 nm thick. The composition of the metal elements in the films was determined by both the atomic absorption spectrometry and the inductively coupled plasma-emission spectrometry of a solution, which was prepared by dissolving a film in a HNO_3 solution. The temperature dependence of the resistivity of a film was measured by a direct current (d.c.) four-probe method. The Seebeck effect was measured in the range 100–300 K.

3. Results

Y-doped $CaCuO_2$ films were formed at a suitable substrate temperature (730–790 °C) and at an optimum oxygen flow rate, as shown in Fig. 1. Y-doped $CaCuO_2$ films were formed in a narrow oxygen-flow-rate range at low temperatures and in a wide range of oxygen flow rates at fairly high temperatures. In addition, the optimum flow rate of oxygen increased with increasing substrate temperature (the accurate partial pressure of oxygen near the $SrTiO_3$ substrate was not measured.). The preferable flow rate of oxygen may be governed by the following equilibrium: $2CuO \rightarrow Cu_2O + 1/2O_2$.

In order to prepare Y-doped $CaCuO_2$ films ($x > 0.1$), the molar ratio of vaporized $Y(thd)_3$ to $Cu(thd)_2$ was enhanced up to 0.2. However, the formation of $Ca_{1-x}Y_xCuO_2$ was not confirmed at a vaporized molar ratio, $Y(thd)_3/Cu(thd)_2$, of 0.05 or more.

0022–2461

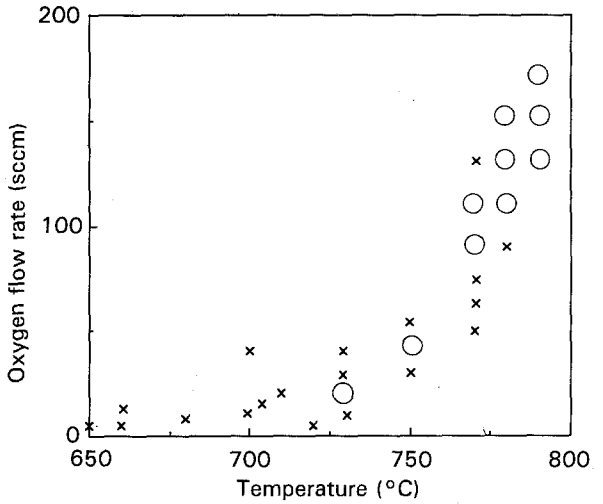

Figure 1 The relationship between the oxygen flow rate and the substrate temperature in the deposition processes of films: (○) the formation of Y-doped $CaCuO_2$ confirmed by XRD, and (×) no formation of $CaCuO_2$.

TABLE I The composition of $Ca_{1-x}Y_xCuO_2$ films deposited on $SrTiO_3$ (1 0 0) substrates

Sample number (*c*-axis)	Substrate temperature (°C)	Vaporized precursors (mol) (Deposited metal elements (mol))		
		Cu	Y	Ca
1(0.3183 nm)	734	6.1×10^{-6} (3.4×10^{-7})	3.0×10^{-8} (4.1×10^{-9})	7.1×10^{-6} (4.1×10^{-7})
2(0.3183 nm)	750	6.5×10^{-6} (1.9×10^{-7})	1.5×10^{-8} (2.3×10^{-9})	6.9×10^{-6} (2.4×10^{-7})
3(0.3180 nm)	750	6.8×10^{-6} (2.1×10^{-7})	3.0×10^{-8} (4.1×10^{-9})	7.1×10^{-6} (2.2×10^{-7})
4(0.3183 nm)	770	6.5×10^{-6} (1.4×10^{-7})	1.5×10^{-8} (2.9×10^{-9})	6.6×10^{-6} (1.8×10^{-7})
5(0.3182 nm)	780	1.1×10^{-5} (2.6×10^{-7})	3.0×10^{-8} (3.3×10^{-9})	1.0×10^{-5} (3.4×10^{-7})

For several films exhibiting intense reflections of $CaCuO_2$, the number of moles of vaporized chelates and of the metal elements contained in these films are listed in Table I. As seen in Table I, the content of Y atoms is less than a few per cent, which is approximately close to the vaporized molar ratio, $Y(thd)_3/Cu(thd)_2$.

Fig. 2 shows the X-ray diffraction (XRD) patterns of the Y-doped $CaCuO_2$ film labelled 4. The XRD pattern is almost the same as in $CaCuO_2$, except for a slight difference in 2θ [3]. Thus, reflections at 2θ of 28.0 and 57.9 can be indexed to (0 0 1) and (0 0 2) of Y-doped $CaCuO_2$. Thus, the *c*-axis of the film is preferentially oriented perpendicular to the substrate surface. The *c*-axis of the Y-doped $CaCuO_2$ film labelled 4 is estimated to be 0.3183 nm. The *c*-axis values of the other films range from 0.3180 to 0.3183 nm. These values for the *c*-axis are slightly shorter than those of non-doped $CaCuO_2$ ($c = 0.3188$ nm) [3]. Thus, the Y-doping of $CaCuO_2$ results in shortening of the *c*-axis. Such shortening of the *c*-axis by electron doping has been observed in n-type superconductors, for example $Nd_{2-x}Ce_xCuO_4$. Information on the *a*-axis of Y-

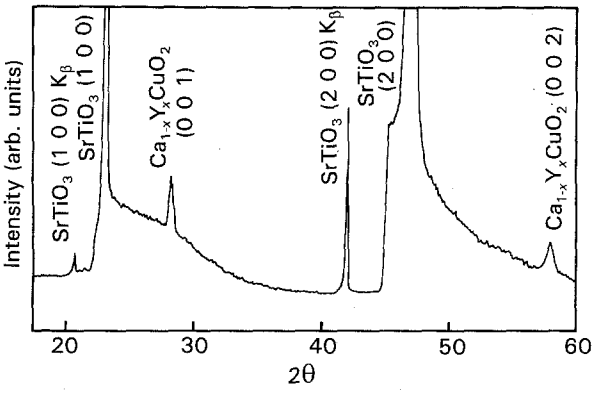

Figure 2 XRD of the Y-doped $CaCuO_2$ film labelled 4 in Table I (CuK_α).

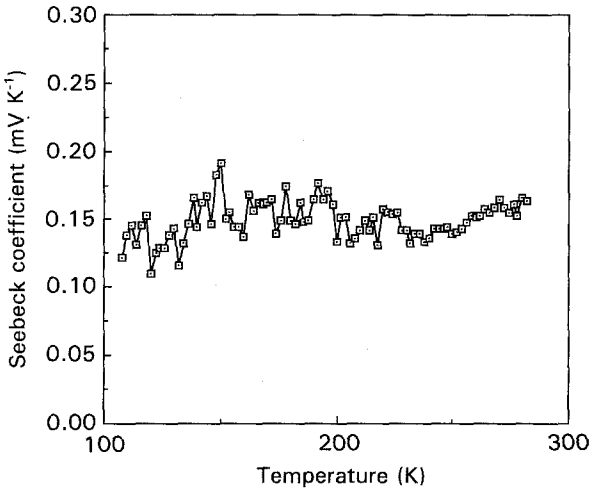

Figure 3 Plots of absolute values of the Seebeck coefficient against temperature for the Y-doped $CaCuO_2$ film labelled 4 in Table I. The Seebeck coefficient is negative.

doped $CaCuO_2$ could not be obtained because the (1 1 0) and (2 2 0) reflections of $CaCuO_2$ were not observed in XRD of films deposited on $SrTiO_3$ (1 1 0) substrates.

All Y-doped $CaCuO_2$ films prepared in the present work exhibit negative Seebeck coefficients at temperatures lower than 270 K. In Fig. 3, the Seebeck coefficient for the film labelled 4 is plotted as a function of temperature. The Seebeck coefficient is negative in the temperature range 110–270 K, so the carriers of these Y-doped $CaCuO_2$ films are electrons, which may be generated by the substitution of Y atoms for Ca sites in $CaCuO_2$. It should be noted that the Seebeck coefficient is nearly constant in the range of 270–100 K.

Fig. 4 shows plots of the resistivity, ρ, against the temperature, *T*, of the Y-doped $CaCuO_2$ films labelled 3 and 4. For these films, the temperature dependence of the resistivity is weak at temperatures higher than 50 K, whereas the resistivity increases remarkably at temperatures higher than 50 K. Unfortunately, no drastic decrease in the resistivity is observed for films 3 and 4 at temperatures higher than 12 K; no superconductivity is found for the Y-doped $CaCuO_2$ films at temperatures higher than 12 K. The temperature dependence of the resistivity shown in Fig. 4 has been observed for lightly doped $La_{2-x}Sr_xCuO_2$ ($x < 0.06$)

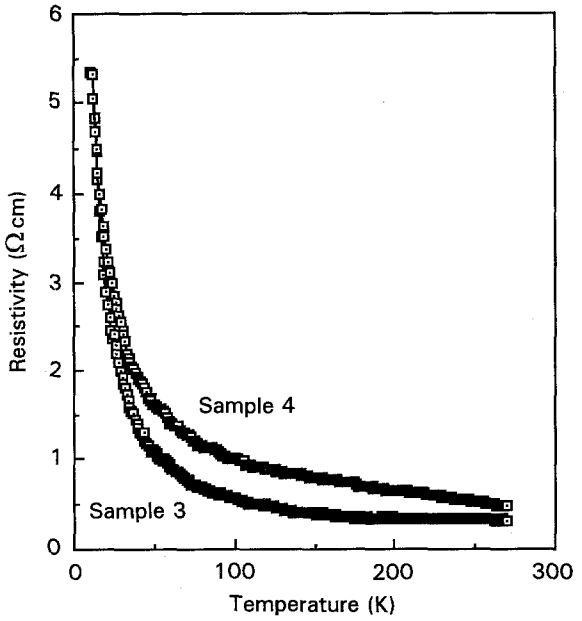

Figure 4 Plots of ρ against T for the Y-doped $CaCuO_2$ films labelled 3 and 4 in Table I.

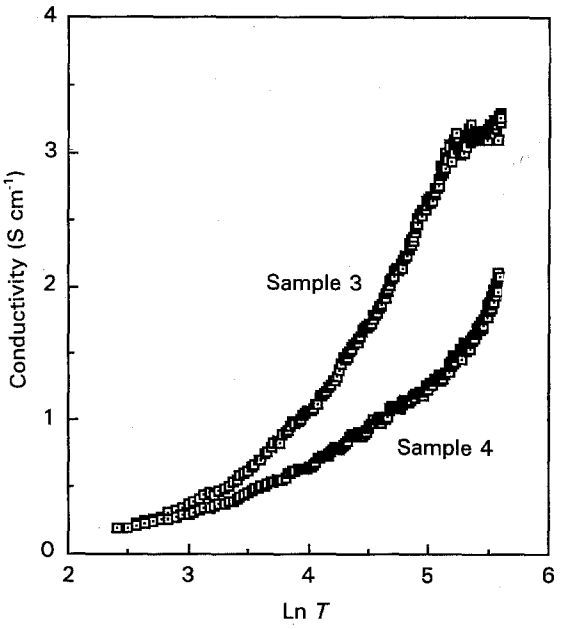

Figure 5 Plots of σ against ln T for the Y-doped $CaCuO_2$ films labelled 3 and 4 in Table I.

and superconductivity emerged with further hole-doping [4]. Thus, superconductivity might appear for a Y-doped $CaCuO_2$ film with a higher carrier concentration if the problem of the low solubility of Y atoms in $CaCuO_2$ is overcome.

4. Discussion

As seen in Table I, the Y-content in $CaCuO_2$ is a few per cent. This result implies that the solubility limit of Y-atoms in $CaCuO_2$ is of the order of a few per cent. The ionic radius of Y^{3+} ions is close to that of Ca^{2+} ions, so that the substitution of Y^{3+} ions for Ca^{2+} ions is expected to occur to some extent, from a crystallographic viewpoint. In fact, superconductivity was found at 65 K for $Pb_2Sr_2Y_{1-x}Ca_xCu_3O_8$ ($x = 0.5$) [5]. Thus, the low solubility of Y atoms in $CaCuO_2$ may be due to the instability of $CaCuO_2$, because $CaCuO_2$ is not synthesized at 1 atm.

The Seebeck coefficient, S, for non-degenerate semiconductors is written as $S = (k/q)(5/2 + r + E_f/kT)$, where E_F is the Fermi energy with respect to the bottom of the conduction band and r is a constant dependent on the scattering mechanism. The temperature independence of the Seebeck coefficient shown in Fig. 3 means the zero-Fermi-energy: carriers of Y-doped $CaCuO_2$ are degenerate. In general, the zero Fermi energy is realized when the carrier concentration is larger than the effective state density of the conduction band. Under this condition, the Fermi level is located in the conduction band and thus the carrier concentration is independent of temperature. As seen in Fig. 4, however, the resistivity is remarkably high near 50 K. Such a temperature dependence of the resistivity is not typical of normal degenerate semiconductors. The localization of carriers occurs for conductors containing a large amount of the random potential (disordered conductors), even if an appreciable state density is present at the Fermi level. The localization of carriers is called Anderson localization [6]. According to a recent theory of Anderson localization, the localization of carriers always occurs for the case of two-dimensional conductors, and occurs in the case of three-dimensional conductors with a carrier density less than a critical value. In the Anderson localization of a weakly localized regime, the conductivity consists of a term proportional to ln T for a two-dimensional conductor [7]. For instance, a linear relationship was observed in plots of the conductivity, σ, against ln T for $Nd_{2-x}Ce_xCuO_4$ films with low carrier densities [8]. In Fig. 5, the conductivity, σ, of films 3 and 4 is plotted as a function of ln T. No linear relationship is seen in Fig. 5. Accordingly, the localization of carriers of the Y-doped $CaCuO_2$ films labelled 3 and 4 is not in accordance with a weakly localized regime of two-dimensional conductors. In the weakly localized regime of three-dimensional conductors, the conductivity contains a term proportional to temperature [9]. In Fig. 6, the conductivity, σ, is plotted as a function of T. In Fig. 6, it seems that the conductivity is proportional to T at temperatures lower than 180 K. However, zero conductivity at $T = 0$ is anticipated from an extrapolation of the σ versus T plot. Thus, the temperature dependence of the conductivity shown in Fig. 5 is not explained by the weak localization in three-dimensional conductors, in which a non-zero minimum conductivity should be obtained at $T = 0$.

Although an explicit formula for strong localization at finite temperatures is not presented, the temperature dependence of the conductivity can be qualitatively expressed by variable range hopping in which the conductivity, σ, is given by $\sigma(T) = \sigma_0 \exp[-(T_0/T)^{1/(d+1)}]$, where d is the dimensionality [10]. In Figs 7 and 8, ln σ is plotted as a function of $T^{-1/3}$ and $T^{-1/4}$, respectively. A good linear relationship is seen in the plots of ln σ against $T^{-1/4}$. A linear relationship has been observed in plots of ln σ against $T^{-1/3}$ for $Nd_{2-x}Ce_xCuO_4$ [8]. According to the theory of variable range hopping [10],

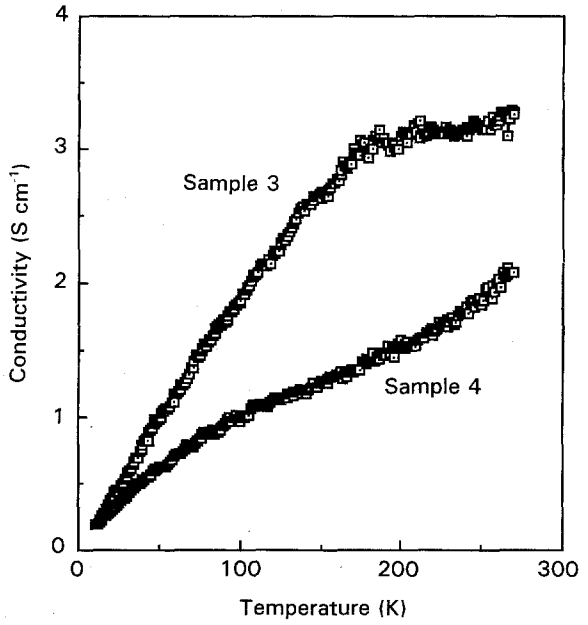

Figure 6 Plots of σ against T for the Y-doped $CaCuO_2$ films labelled 3 and 4.

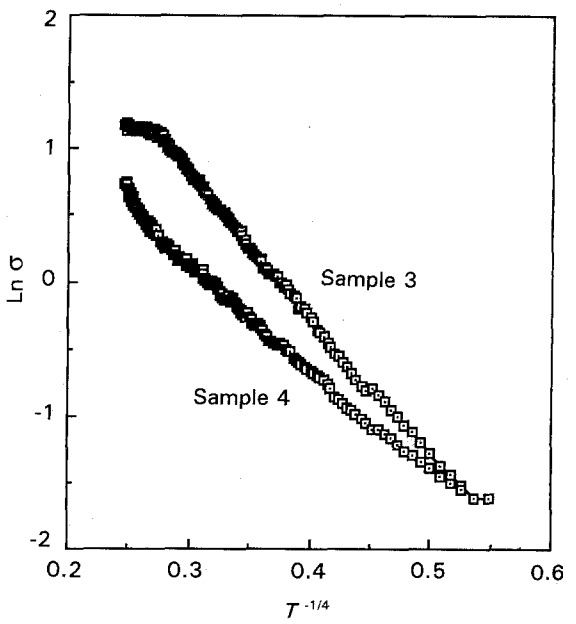

Figure 8 Plots of ln σ against $T^{-1/4}$ for the Y-doped $CaCuO_2$ films labelled 3 and 4.

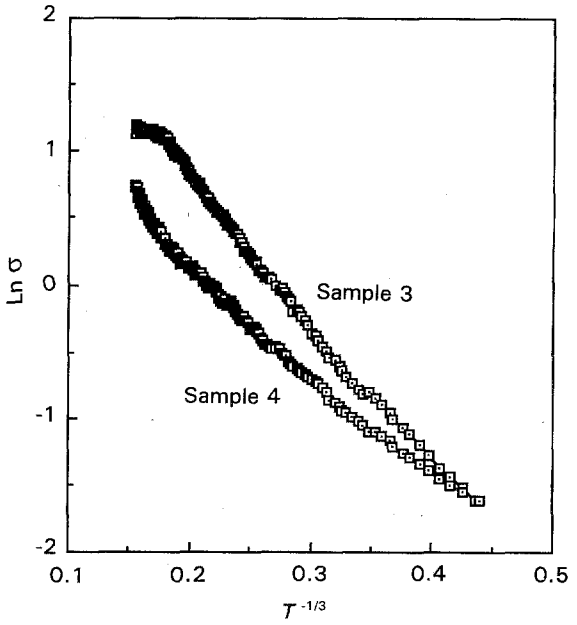

Figure 7 Plots of ln σ against $T^{-1/3}$ for the Y-doped $CaCuO_2$ films labelled 3 and 4.

$Nd_{2-x}Ce_xCuO_4$ is a two-dimensional conductor, whereas Y-doped $CaCuO_2$ is a three-dimensional conductor. This difference may be attributable to the lack of blocking layers between the CuO_2 sheets in the $CaCuO_2$ structure. Another explanation is attributed to the many defects in the *ab*-plane, because a linear relationship was found in plots of ln ρ against $T^{-1/4}$ for $La_{2-x}Sr_xCuO_4$ ($x < 0.06$) which has blocking layers between the CuO_2 sheets [4]; two-dimensional conduction is interrupted by defects in the *ab*-plane, and then the conduction along the *c*-axis is not neglected.

As mentioned above, strong localization occurs for disordered two-dimensional metals and for disordered three-dimensional metals with low carrier densities as the temperature is lowered. Besides these disordered metals, strong localization is expected for charge transport through an impurity band in heavily doped semiconductors [10]. As seen in Table I, if 2% of the Ca^{2+} ions in $CaCuO_2$ are substituted by Y^{3+} ions, the state density of the impurity levels due to Y atoms is estimated to be 4.2×10^{20} cm^{-3}. This value of the state density is insufficient to form an impurity band over the $CaCuO_2$ crystal. Under this condition, variable range hopping is a predominant process at lower temperatures. The Y-doped $CaCuO_2$ films exhibit sharp reflection peaks in the XRD patterns, so that it seems that the Y-doped $CaCuO_2$ films are not corresponding to disordered metals. The origin of the strong localization of the Y-doped $CaCuO_2$ films may be related to the impurity band. Recently, the temperature dependence of ln ρ against $T^{-1/(d+1)}$ has been explained by the localization of bosons [11]. To explain the present work by bosons localization, it is necessary to measure the effects of the magnetic field on the resistivity.

References

1. M. G. SMITH, A. MANTHIRAM, J. ZHOU, J. B. GOODENOUGH and J. T. MARKERT, *Nature* **351** (1991) 549.
2. M. TAKANO, Y. TAKEDA, H. OKADA, M. MIYAMOTO and T. KUSAKA, *Physica C* **159** (1989) 375.
3. K. KOBAYASHI, Y. ISHIHARA, S. MATSUSHIMA and G. OKADA, *Jpn. J. Appl. Phys.* **30** (1991) L1931.
4. H. TAKAGI, T. ITO, S. ISHIBASHI, M. UOTA, S. UCHIDA and Y. TOKURA, *Phys. Rev. B* **40** (1989) 2254.
5. R. J. CAVA, B. BATLOGG, J. J. KRAJEWSKI, L. W. RUPP, L. F. SCHNEEMEYER, T. SIEGRIST, R. B. VAN DOVER, P. MARSH, W. F. PECK Jr, P. K. GALLAGHER, S. H. GLARUM, J. H. MARSHALL, R. C. FARROW, J. V. WASZCZAK, R. HULL and P. TREVOR, *Nature* **336** (1988) 211.
6. E. ABRAHAMS, P. W. ANDERSON, D. C. LICCIAR-

DELLO and T. V. RAMAKRISHNAN, *Phys. Rev. Lett.* **42** (1979) 673.
7. L. P. GORKOV, A. Z. LAIRKN and D. E. KHMELNITZKII, *JETP Lett.* **30** (1979) 248.
8. S. TANDA, M. HONMA and T. NAKAYAMA, *Phys. Rev. B* **43** (1991) 8725.
9. G. A. THOMAS and A. KAWABATA, *ibid.* **26** (1982) 2113.
10. N. F. MOTT, *Rev. Mod. Phys.* **50** (1978) 203.
11. M. P. A. FISHER, *Phys. Rev. Lett.* **65** (1990) 923.

Received 17 November 92
and accepted 17 May 93